# Development of a Laser-Based Water Level Sensor for Fine-Scale Ecohydrological Measurements

Joshua Benjamin, Dr. David Kaplan
Dept. of Environmental Engineering Sciences
University of Florida
Gainesville, FL, USA

*Abstract*— **Evapotranspiration (ET) is a critical component of the global water cycle, but one that is difficult to estimate due in part to a lack of accurate and affordable sensor technology. One low-cost approach to measuring site-specific ET in areas where the water table is close to the surface is to take advantage of the diurnal fluctuations in surface water and groundwater driven by ET. This method requires highly sensitive measurement to accurately quantify water table variation. The goal of this work is to develop and test a laser-based water level sensor (LB-WLS) to improve the estimate of ET via diurnal variations in water level. The LB-WLS was compared against traditional total pressure transducers (TPT) in both laboratory and remote settings. The LB-WLS was found to have lower residual noise, with an average Root Square Error (RSE) of 0.05±0.04 cm, compared to 0.19±0.16 cm for the TPT sensor. While sensor development is ongoing, this level of performance represents a major improvement in fine-scale monitoring of surface water and groundwater.**

***Keywords— Sensors, Water Level, Evapotranspiration, Hydrology, Well, Bluetooth***

## I. PREMISE

Evapotranspiration (ET) is a crucial component in the global hydrologic balance. Globally, land-based ET returns about 60% of incoming precipitation [1] to the atmosphere and is strongly influenced by land use and water coverage. This is especially notable in Florida, where ET can account for 70-95% of the incoming precipitation [2]. Given these high rates, it is crucial that ET be accurately quantified, especially in the context of the projected water scarcity across the southeastern United States and the world [2].

Numerous methods exist for measuring and modeling ET, including the Bowen ratio energy balance method, the eddy covariance method, and the simultaneous heat and water model (SHAW) [3]. However, these methods are often limited by both data availability and cost[1], which limit their applicability [4]. One low-cost approach to measuring site-specific ET is to take advantage of the diurnal variations in groundwater levels that exist in locations where the water table is close to the surface [5]. Critically, this method requires high-resolution data to accurately quantify daily water table or surface water level fluctuations [6].

### A. Current Technology

Currently, the most widely used water level sensor used for ecohydrological measurements are total pressure transducers (TPT). These sensors are reliant on atmospheric pressure compensation using separate barometric pressure transducers (BPT). TPT-BPT pairs work by measuring hydrostatic pressure by attaching a series of strain gauges to a pressure membrane, which can generate an electrical resistance change that is proportional to a change in air or water pressure [7], and typically have an accuracy of ±0.4 cm, and a resolution of 0.14 cm. While reliable, this measurement technique has its limitations, as TPT-BPT pairs are prone to errors based on installation location and media, differences in atmospheric and water temperatures, variations in solar radiation, and long equilibration times [7].

Additionally, even when installed correctly, they are still prone to error (>1 cm) due to factors including moisture accumulation and differential heating across the system under ambient conditions [6]. Given these drawbacks, existing water level sensor systems make it difficult to achieve the fine-scale resolution observations of water levels necessary to elucidate ET, particularly in surface water systems [6] or during times with low ET rates (cloudy days, winter).

### B. New Technology

To help mitigate the effects of these errors, we developed and tested a laser-based water-level sensor (LB-WLS)[2]. The laser used is a Leica DISTO™ E7100i laser distance meter (LDM). This LDM utilizes the phase shift method of laser distance measurement. In the phase shift method, the optical power of the laser beam is modulated with a constant frequency. Measurements are conducted by sinusoidally modulating the dc current of the laser diode, which in turn affects the transmitted light intensity. After the beam is reflected off the target, a photodiode collects the reflected beam, which creates a photoelectric current [9]. Distance, D, can be obtained by measuring the phase shift between the photoelectric current (the measurement signal) and the

This work was made possible thanks to a scholarship from the University of Florida McNair Scholars Program, as well as the University of Florida University Scholars Program.

[1]Measurement systems can run anywhere from $4,000 – $40,000 [4] .

[2]Another existing technology that operates in similar fashion to the LB-WLS is ultrasonic sensors. Ultrasonic sensors that are suitable for ecohydrological measurements are accurate up to 1.25 cm [8], which is less precise than the TPT-BPT. Therefore, they were not compared against in this investigation.

978-1-5386-0452-6/17/$31.00 ©2017 IEEE

modulated emitted signal (the reference signal) using Equation (1),

$$D = \frac{c}{2f} \cdot \frac{\Delta\varphi}{2\pi} \quad (1)$$

where c is the speed of light, f is the modulation frequency, and Δφ is the phase shift between the measurement signal and the reference signal [10].

For this process to function effectively, the phase shift Δφ must be measured accurately to obtain a precise distance measurement. To improve phase measurement accuracy, the auto-digital phase measurement will usually process the signals with a heterodyne method, which can convert the two high-frequency signals into low-frequency signals [11]. These techniques help improve the signal to noise ratio (SNR) of the measurement and enable mm-range resolution at distances of 0.0015 to 60.96 m with noncooperative targets[3]. This gives the LB-WLS an expected advantage over traditional water level measurement technologies that rely on variations in pressure and temperature, as the device's optical basis should enable it increased stability in dynamic environments. Due to these parameters, a standard LDM is accurate to ±0.15cm and resolves to the nearest 0.01 cm, which is 2.6 times as accurate and 14 times the resolution of the TPT-BPT pair.

Due to this enhanced accuracy, as well as the advantages that come from an optical-based measurement system, we hypothesize that the LB-WLS will have higher levels of accuracy and resolution than current water level sensing technology by significantly lowering residual error of measurement. Greater measurement accuracy may be able to address issues such as how vegetative cover effects ET in wetland environments compared to open water, and how to best manage pine forests for enhanced water availability [2], allowing landowners to make more informed decisions on water usage and land coverage. The hypothesis was tested by comparing the LB-WLS to the TPT-BPT pair in an upland pine forest in Hawthorne, Florida.

## II. PROCESS

### A. Sensor Design

The design comprises three components: a laser distance meter (LDM), a microcontroller, and a floating target platform (FTP).

#### 1) Laser Distance Meter

The laser rangefinder used for the LB-WLS was a Leica DISTO™ E7100i (Disto) by Leica Geosystems (St. Gallen, Switzerland). The Disto was chosen primarily for its low cost ($149.00), its high measurement accuracy (±0.15 cm) and resolution (0.01 cm), as well as the fact that is IP54 certified[4]. The Disto can send distance measurements via Bluetooth® SMART, which makes it one of the least expensive Bluetooth LDM's available on the market [14]. The ability to send measurements via Bluetooth® SMART is particularly important, as it is this characteristic that allows the recording of data on a microcontroller.

Modifications were made to the Disto to enable it to function in a remote environment. These modifications involved altering the power supply to make the Disto externally powered and creating a casing for the Disto to be placed in the field. Modifications included two iterations:

The first iteration involved connecting the Disto to a custom-built voltage regulator circuit board that down-stepped the voltage from 5V to 3V so that the Disto could be USB powered. For the casing, a well cap was constructed using 1.5 in. thick PVC pipe. The first iteration was used in the initial field trial, and was relatively successful, except for stability and heating issues.

The second iteration involved modifying the power supply by replacing the circuit board with a buck converter. The buck converter was chosen due to its ability to output less heat than a voltage regulator, and its small size, which enabled it to be placed inside of a custom 3D-printed battery casing inside of the Disto while still being connected to a USB cable. The second iteration of the well casing was reinforced using bolts that were drilled into the casing, which hold the Disto in place, creating a reinforced laser housing. Furthermore, an access hatch was added so that the laser could be turned on while inside of the well (Figure 1).

Figure 1. The experimental setup the field trial. *The laser is located inside of the well on the left, which was installed in the Longleaf Flatwoods Reserve in Hawthorne Florida. The CHIP is inside the case in the right corner, which is connected to an AGM car battery.The BPT is in the well in the rear.*

[3]A non-cooperative target is a target in which no laser beacon is provided directly by the target for wavefront sensing. This means that no laser beacon is available from the target except that obtained from the target itself or from the atmosphere [12].

[4]IP54 certification implies that a device is protected from limited dust ingress and protected from water spray in any direction (DSM&T CO., INC., 2011) [13]. These protections make the Disto ideal for field deployment.

*2) Microcontroller*

The initial microcontroller that was used for the design was a Raspberry Pi 2 Model B (Pi 2B) by the Raspberry Pi Foundation (Caldecote, United Kingdom). The Pi 2B was chosen for its low cost ($35.004), small size, low power usage, versatility, and high processing power. The Pi 2B was set up to run the latest distribution (at the time) of Rasbian (Rasbian Jessie 4.1, March 2016).

Bluetooth SMART was used to communicate between the Disto and the Pi 2B. This was done by first connecting a Bluetooth® 4.09 radio to the Pi 2B, which in this case was a Panda Wireless Bluetooth® 4.0 USB Nano Adaptor. This adapter allows the Pi 2B to receive a Bluetooth® 4.0 signal. The Bluetooth® profile description for the Disto was provided by Leica Geosystems. The BlueZ[5] protocol stack was installed on the Pi 2B, and it was used to translate the Bluetooth® signals that were sent between the Disto and the Pi 2B during operation. These signals were a combination of indicate and write without response commands.

A program called Laser.py was written to control both devices using Python. Disto. Laser.py records input variables from the user, including measurement frequency and start and end times, and it is designed to automatically record the data that is generated during the measurement period. The UUIDs (universally unique identifiers) that were transmitted were found to broadcast in hexadecimal format and could be recorded once they were converted into strings by the program.

During the field trials, the Pi 2B was replaced with a CHIP by Next Thing Co. (Oakland, California). The reason for this was because the CHIP had lower power consumption, and was paired with a portable touchscreen and keyboard for ease of deployment. However, the CHIP still consumes a large amount of power and is in line to be replaced with a Pycom (Guilford, United Kingdom) LoPy, which is an ultra-low power python-based microcontroller, that can be remotely controlled using a LoRa radio. Before the CHIP can be replaced with the LoPy, Laser.py will need to be rewritten to operate using micropython instead of python.

*3) Floating Target Platform*

A floating target platform is required to take water level measurements due to the need to provide a stable non-cooperative target. The FTP was designed using the AutoDesk 123D design software package and 3-D printed using Polylactic Acid (PLA) on a Makerbot printer. The main governing equation utilized in the design process was the buoyancy equation (Equation 2),

$$F_b = \gamma_{fluid} \forall_{body} \quad (2)$$

where $\gamma_{fluid}$ stands for the specific weight of the fluid, and $\forall_{body}$ stands for the volume of the submersed body.

The FTP went through five design iterations and was designed to be used in a well with 1.25-in Schedule 40 PVC Pipe. The Mk-III and the Mk-V showcased in Figure 2.

[5]BlueZ is the official Linux Bluetooth® protocol stack and provides support for the core Bluetooth® layers and protocols

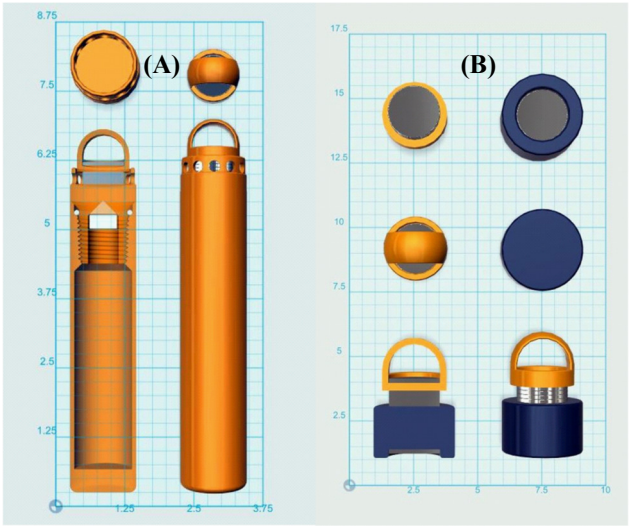


Figure 2. FTP Designs: (A) The FTP Mk-III. *The top left is the target platform, the top right is the Magnetic retriever, the bottom left is a cutaway view showing the central cavity, screw-cap, magnets, and O-ring, and the bottom right is the entire assembly.* (B) The final design for the FTP (FTP Mk-V). *The top left is the bottom of the retriever, the mid-left is the top of the retriever(the target surface), and the bottom left is a cutaway view showing the magnet inside of the floater. The top right is the bottom of the floater, the mid right is the top of the floater, and the bottom right is the entire assembly.*

The first four designs (Mk-I – Mk-IV) featured a cylindrical tube with a flat firing platform on top and a large air-filled cavity in the center to make the platform stable and buoyant. Later revisions (Mk-III+) incorporated a magnetic retrieval system by incorporating two 0.5 in diameter neodymium magnets.

The fifth design (Mk-V) cut the large air-filled cavity from the body and shifted to a lower-density construction. This was done after the initial field trial, where it was discovered that the height of the Mk-IV led to inconclusive results whenever the water table decreased, as the floater ended up getting stuck in the well. Due to this, the floater's height shifted from 5 inches to 1 inch, which in turn led to enhanced stability and a lower center of gravity.

The FTP retriever itself underwent two design revisions, with the first design relying on super glue to attach the magnets to the retriever, and the second design implementing magnets on both sides of the retriever's central disk to prevent the magnets from slipping. Figure 2 showcases the Mk-III and the Mk-V respectively, with the retriever shown in both images for scalar comparison.

### *B. Experimental Setup*

The tests took place in an upland section of the Longleaf Flatwoods Reserve in Hawthorne Florida. The installation of the well occurred in July 2016. This was done by first digging a hole with a hand auger to approximately 2m deep. Next, a knitted filter sock was placed over a 2m long segment of 1.25 in Schedule 40 slotted PVC and secured with zip ties. The hole was then bailed out using the auger to prevent the well from

collapsing, and then the PVC pipe was inserted into the well hole, and secured using sand and bentonite clay. Initial field trials were conducted to optimize the functionality of the LB-WLS and did not involve comparison with a TPT-BPT pair.

The first series of trials were conducted in the summer and fall of 2016 and involved the MK_III FTP, the Pi 2B, and the first iteration of the remote LDM. Both the circuit board and the Pi 2B were placed inside of an external waterproof container and connected to a 12V car battery for power. Since there was no way for the Pi 2B to be programmed in the field, an automatic script was placed on the Pi 2B to Laser.py activate whenever the PI 2B turned on, which enabled the test to be conducted with minimal equipment. The setup was left in the field for a week and was then retrieved and sent back to the lab for analysis.

During the late fall of 2016, the field design was finalized. A long-term trial was conducted from December 6th, 2016, to December 29th, 2016, with a visit on December 15th, 2016, to inspect the sensors and replace the battery powering the LB-WLS. In this trial, the LB-WLS was compared to a HOBO Water Level Data Logger (accuracy = ± 0.4 cm, resolution = 0.14 cm) by Onset (Bourne, Massachusetts), which was mounted in a separate well approximately 5 feet away that was constructed using the same method. This trial used the MK-V floater, the CHIP, and the reinforced laser housing. After December 2016, the trial was conducted until the sensor ran out of battery.

### C. Data Analysis

To calculate the diurnal rise and fall of the water table, the data from each sensor were compensated to generate a comparable basis. The data from the HOBO logger was compensated by first subtracting the pressure from the barologger from the pressure transducer (both in kPa), and then using this value to solve for height using Equation (3),

$$p = \rho g h \tag{3}$$

where p is pressure, ρ is density, g is the gravitational constant (9.806 m/s$^2$), and h is the height of the water above the pressure transducer. After this, this value was subtracted from the distance from the ground to the transducer to get the water level. Similarly, to get the water level from the LB-WLS, subtract the distance from the LB-WLS to the ground from the given measurement.

Actual ET can be determined using Equation (4),

$$ET = S_y \times \left(\frac{\Delta s}{t} + R\right) \tag{4}$$

where ET is the rate of groundwater consumed by evapotranspiration averaged over a 24 hour period [L], $S_y$ is the soil specific yield, Δs is the daily change in storage that is calculated as the daily net rise or fall of the water table [L], t is time [T], and R is the net inflow rate [L/T] determined from the hourly rate change in water table elevation during the hours from 12 AM to 5 AM when ET is assumed to be negligible [15].

A particularly uncertain part of the ET estimate is the choice of appropriate specific yield. In this investigation, the depth-compensated specific yield was utilized, based on an equation analogous to that used by Duke (1972) [16]:

$$S_y^{d-comp}(d) = \theta_s - \left[\theta_R + \frac{\theta_s - \theta_R}{[1 + (\alpha|d|)^n]^m}\right] \tag{5}$$

where $S_y$ is specific yield, $\theta_s$ is the water content at saturation, $\theta_R$ is the residual water content, d is the depth to the water table [L], and α, n, and m are van Genuchten coefficients, with α having units of [1/L]. Note that these values can be found in Table 1 in Loheide et al (2005) [15].

The accuracy of the water level reading between the LB-WLS and the HOBO was then compared by first calculating the RSE (Root Square Error) of the difference between the measured values and the calculated value based on the net inflow rate [L/T] determined from the hourly rate change in water table elevation during the hours from 12 AM to 5 AM (R) (Figure 3). These values were then tabulated and compared using a two-tailed t-test at a 95% confidence level.

The measured ET values were compared by graphing them against a 1:1 basis, to see which device produced higher overall estimates. Actual ET was compared to potential evapotranspiration (PET), which is the amount of evaporation that would occur from a well-vegetated surface when moisture supply is not limiting [17]. PET values were extracted from the Florida Automated Weather Network (FAWN). The values used were from Citra, Florida, and PET was calculated using the FAO (Food and Agriculture Organization of the United Nations) 56 Penman-Monteith Equation [18]. ET:PET ratios for both devices were calculated, and compared based on mean and standard deviation.

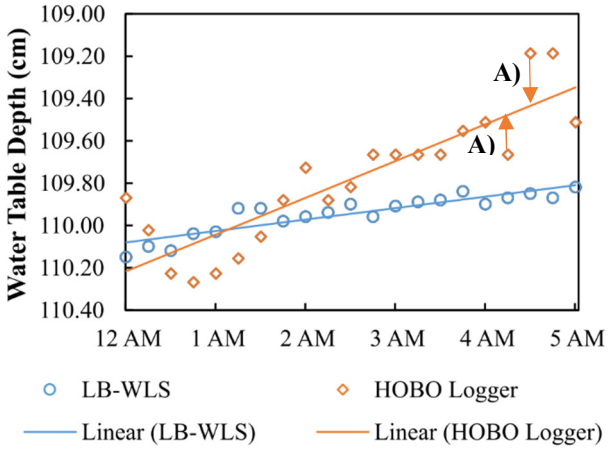


Figure 3. RSE value calculation. *To calculate the RSE values, the slope of the hourly rate change in water table elevation during the hours from 12 AM to 5 AM (R) was extracted from the data, and then the difference between the slope and the measured value was determined for each data point (A).*

## III. OUTCOME

### A. Initial Field Trial

The results from the initial field trial are presented in Figure 4. This trial was solely for testing the LB-WLS hardware, and so did not involve any comparisons with a TPT-BPT pair.

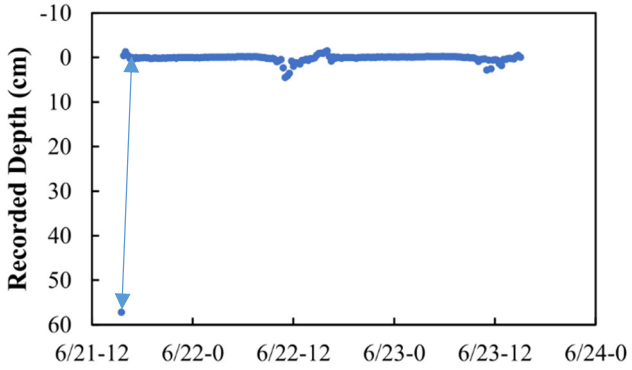


Figure 4. Results from the initial field trial. *Due to a lack of stability in the initial setup, the laser ended up recording the distance to the side of the well for most of the trial. Also, around noon of each day, there was a periodic fluctuation in the distance from the laser to the well. The reason for this is unknown, but it may have been due to high temperatures disrupting the measurement accuracy.*

### B. Comparison with the HOBO Logger

From December 6, 2016, to December 29, 2016, the LB-WLS was compared with an Onset HOBO logger. The results are shown in Figures 5 and 6, with the distance to the water table recorded in cm. Precipitation data was retrieved from the NOAA Climatological Data for Gainesville Area, FL.

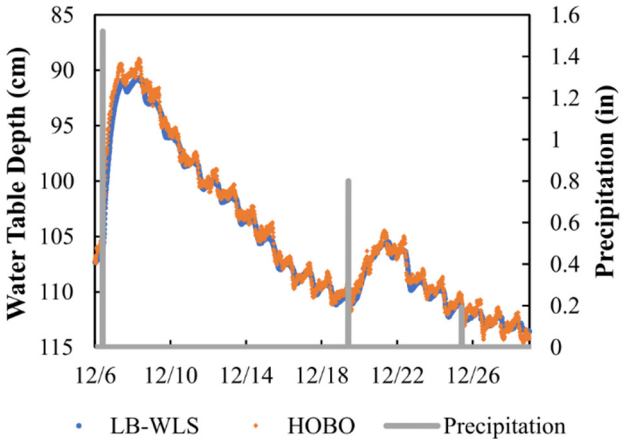


Figure 5. Results from the comparative field trial. *The water level signal for both trials graphed against precipitation, where the water table rises after it rains. It can also be seen that the water table has a diurnal signal, where it falls during the day, and rises at night due to subsurface inflow.*

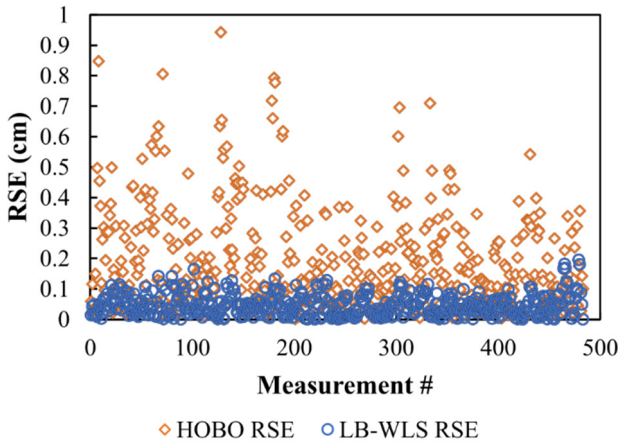


Figure 6. The results from the comparative field trial. *The RSE difference between the measured data and the slope of the net inflow rate (R). Note that the LB-WLS has on average a lower RSE value.*

As can be seen in Figure 6, the LB-WLS has a lower average RSE value, at 0.05±0.04 cm, vs the average RSE of the HOBO Logger, at 0.19±0.16 cm. For a more complete analysis, Table 1 shows the RSE data from each device for each post-precipitation period, with a post-precipitation period starting the day after a precipitation event, and ending the day before the next precipitation event.

TABLE I. RSE VALUES (CM)

| | **Laser Based Water Level Sensor** | | | **Total Pressure Transducer-Barometric Pressure Transducer** | | |
|---|---|---|---|---|---|---|
| ***Dates*** | ***Minimum*** | ***Maximum*** | ***Mean*** | ***Minimum*** | ***Maximum*** | ***Mean*** |
| 12/7-12/13 | 0.00 | 0.12 | 0.05 | 0.02 | 0.59 | 0.23 |
| 12/15-12/18 | 0.00 | 0.11 | 0.04 | 0.01 | 0.38 | 0.14 |
| 12/20-12/24 | 0.00 | 0.10 | 0.04 | 0.02 | 0.51 | 0.19 |
| 12/26-12/28 | 0.00 | 0.13 | 0.06 | 0.02 | 0.39 | 0.15 |
| Mean | 0.00 | 0.12 | **0.05** | 0.02 | 0.46 | **0.18** |
| Overall | 0.00 | 0.19 | 0.05 | 0.00 | 0.94 | 0.19 |

*Note.* All values are absolute. The values reported are the mean value of the criteria from each period. "Mean" is the average of the four measurement periods, Mean w/ rain is the mean of every day's criteria, and overall is across every value in the set.

### C. Determination of ET

The ET Values are plotted in Figure 7. Note that the soil was assumed to be sandy clay, due to its prevalence at depth greater than 38.1 cm in southern Alachua County (FDEP, 2013). This led to an average specific yield of 0.0068, with values adjusted using Equation 5. Days with precipitation were excluded from the analysis because of the effect that precipitation has on subsurface flow rates.

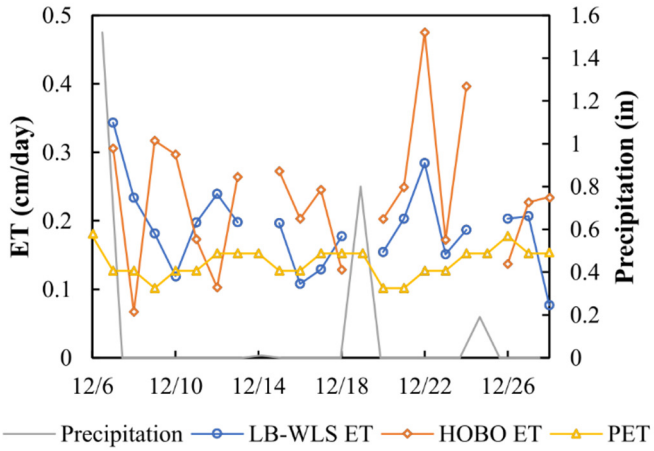


Figure 7. ET estimates from both the LB-WLS and the HOBO Logger. *Days with precipitation were excluded from the analysis.*

The LB-WLS had an average ET rate of 0.19±0.06 cm/day, while the HOBO Logger had an average ET of 0.23±0.10 cm/day. Figure 8 shows the results of comparing the ET readings from the HOBO to the ET readings from the LB-WLS on a 1:1 basis.

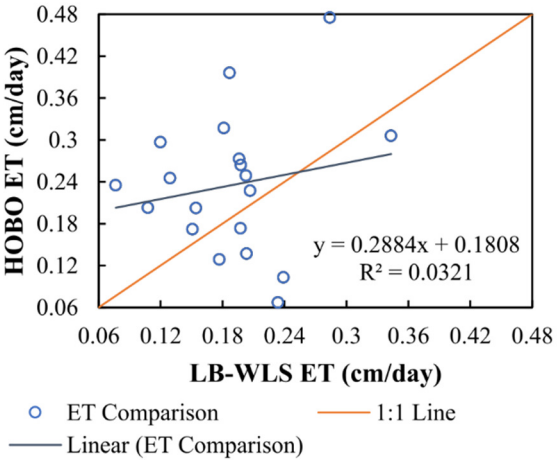


Figure 8. 1:1 Comparisons between HOBO Logger and the LB-WLS ET estimates. *On a 1:1 basis, the ET values from the HOBO are typically larger than the ET values from the LB-WLS. Note that the ET rates in the 0.18 to 0.24 range are closest to the 1:1 basis.*

When comparing ET against PET, a common technique is to use ET:PET ratios (McLaughlin et al., 2013) [2]. Ratios have been calculated for both devices, and are shown in Figure 9.

### *D. Measurement Analysis*

The results from the initial field trial (Figure 4) revealed several things about the initial setup. The most apparent error is the jump from the first measurement to the second measurement, which indicated that the laser most likely shifted within the casing, which was why further trials incorporated a reinforced well casing, as seen in Figure 5.

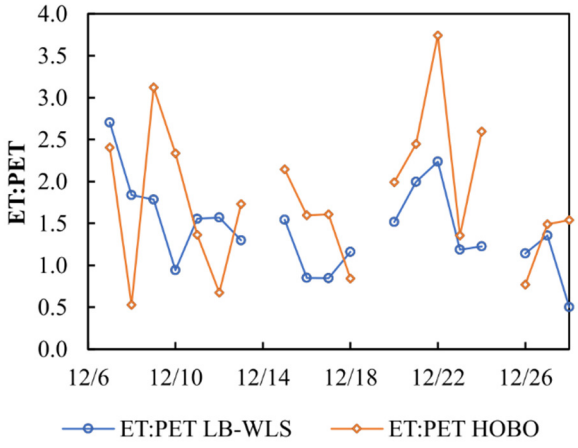


Figure 9. ET: PET comparisons for the HOBO Logger and the LB-WLS *Estimates from both the LB-WLS and the HOBO Logger. Days with precipitation were excluded from the analysis.*

Furthermore, the LB-WLS stopped recording data prematurely, which was due to the initial voltage regulator overheating. This error was corrected in further trials by replacing the voltage regulator with a buck converter[6].

Once the field setup was optimized (see section 4.2.1 for an in-depth power analysis), a long-term comparison trial ran from December 6th, 2016, to December 28th, 2016. Overall, the results indicate that the LB-WLS generated consistently higher resolution water level readings, with an average RSE value of 0.05±0.04 cm, vs the average RSE of the HOBO Logger, at 0.19±0.16 cm. Furthermore, these results were found to be significantly different, with the two-tailed t-test having a P value<0.05. This indicates that the LB-WLS generates consistently higher resolution water level data than the TPT-BPT pair.

In terms of ET measurements, the LB-WLS had an average ET rate of 0.19±0.06 cm/day, while the HOBO Logger had an average ET rate of 0.23±0.10 cm/day. During this time, the average PET rate was 0.14±0.02 cm/day. These values were with a calculated using a sandy clay soil type, which was chosen due to its prevalence in southern Alachua County at depths greater than 38.1 cm [19]. Overall, the ET measurements across both devices were on average higher than the PET measurements, with average ET: PET values being 1.43±0.52 for the LB-WLS, and 1.80±0.82 for the HOBO Logger. While the LB-WLS had values closer to 1 than the HOBO logger, they were still high, which suggests that further investigations in soil characterization may be necessary to improve actual ET estimates.

### *E. Power Analysis*

From December 15, 2016, onward, the LB-WLS was left in the field until the battery died. The battery used was an EverStart Deep Cycle 27DC AGM Battery, and was rated at

[6]This also assisted in making the LB-WLS more waterproof, as the buck converter was not exposed to the elements since it was small enough to fit inside of the laser casing.

12 V and contained 109 Amp Hours @ 1 Amp. Overall, the LB-WLS ran for 301 hours on this battery. The individual power consumptions of each device are recorded in Table 2:

TABLE II. LB-WLS COMPONENT POWER CONSUMPTION

| Device | Minimum (Watt) | Maximum (Watt) |
|---|---|---|
| Disto E7100i | 0.10 | 0.35 |
| Raspberry Pi 2B | 1.25 | 1.40 |
| NTC CHIP | 2.75 | 3.25 |

Note: Each device operates under 5V. Note that while the CHIP uses more power than the Pi 2B, this is with an attached touchscreen and keyboard, which allows for easier data entry and retrieval in the field.

The efficiency of the buck converter that runs between the battery and the devices was found to be 76%. This was done by comparing the input and output wattages on the battery, with the values under both minimum and maximum load for the Disto attached to the CHIP LB-WLS plotted in Table 5. Note that the run time under minimum load was determined using Peukert's Law,

$$t = H\left(\frac{C}{IH}\right)^{k} \quad (6)$$

where t is time [hr], H is rated discharge time [hr], C is capacity [Amp*hr], I is the actual current [Amp], and k is the Peukert constant, which is 1.1 for an AGM battery.

As seen in Table 3, using the current configuration, under minimum load conditions, the LB-WLS is expected to drain a car-sized battery in approximately 2 weeks. This is problematic, as it necessitates semi-weekly visits to the field site to replace the battery. One option is to replace the CHIP with a LoPy, which is a micropython enabled microcontroller produced by Pycom.

Another option is to attach a solar cell to the LB-WLS. Assuming maximum load conditions and an average of 5 peak sun hours per day (Wunderground) at standard AGM1.5G power (1 kW/m2), to get a runtime comparable to the LoPy (>50 days), a 15W solar cell would be required if installed with the CHIP. Various scenarios are graphed in Figure 10, using the equation:

$$IF[E_{n-1} - L + C * S] > E_o:$$
$$THEN\ [E_n = E_0] \quad (7)$$
$$ELSE\ [E_n = (E_{n-1} - L + C * S)]$$

where $E_0$ is the initial capacity of the battery (W*hr), $E_{n-1}$ is the capacity in the previous step, $E_n$ is the capacity in the calculated step, L is the load (W*hr), C is a conditional statement that is equal to 1 during peak sun and 0 when it is not peak sun, and S is the solar cell energy (W*hr).

Note that to get the LB-WLS to run indefinitely, a 20W solar cell would suffice, as it would enable a runtime of 10 years. Furthermore, for the LoPy to run indefinitely (10 years), a 5 W solar cell would more than suffice, with an estimated runtime of 45.4 years.

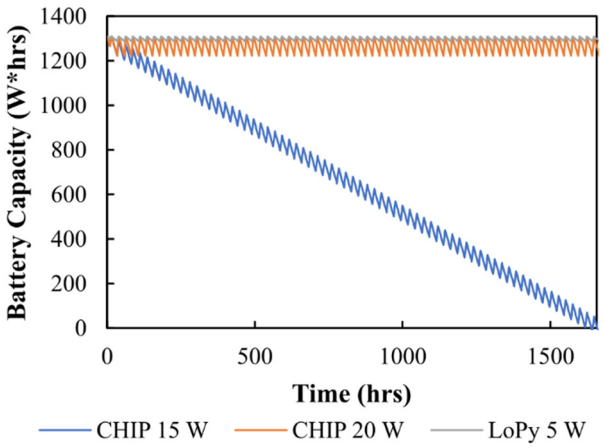


Figure 10. Solar power estimates. *Different scenarios for if solar power were implemented. Note that due to the lower load that the LoPy has, it would be able to run indefinitely on a solar cell that has ¼ the capacity of what it would take to run the CHIP indefinitely.*

TABLE III. LB-WLS COMPONENT POWER CONSUMPTION RELATIVE TO THE CENTRAL BUCK CONVERTER

| Parameter | Maximum Load | Minimum Load | With LoPy[a] |
|---|---|---|---|
| Current (out) [Amp] | 0.72 | 0.62 | 0.17 |
| Power (out) [W] | 3.60 | 3.10 | 0.85 |
| Current (in) [Amp] | 0.40 | 0.34 | 0.09 |
| Power (in) [W] | 4.77 | 4.10 | 1.13 |
| Est. Run Time [hr] | 301 | 355 | 1473 |
| Est Run Time [days] | 12.5 | 14.8 | 61.4 |

*Note*: These values assume that the efficiency (η) of the buck converter is 76%, Vout is 5V, Vin is 12V, and that $P_{in}*\eta = P_{out}$, with P=VI, where P is power (W), V is Voltage (V), and I is current (Amp).

[a]LoPy measurements are potential values based on lab-scale readings and have not yet been experimentally verified.

### F. Error Analysis

In February of 2017, a second field trial was conducted to further assess the capability of the LB-WLS. However, the trial ended up being installed incorrectly, and the data retrieved ended up sending back measurements from the side of the well casing, similar to the results from trial 1. This led to the idea of testing the well inside of a dry well (this well was constructed in the same manner that the other two wells were, except the well casing was not slotted), to assess how the LB-WLS functions when measuring a non-variable target. While it was expected for the data to simply showcase a flat line, it instead exhibited a periodic function, where there was noise every afternoon (Figure 11).

It is currently unknown why the LB-WLS was creating this interference, but it can also be seen that this periodic noise can be found in the other two dry trials. Some possible explanations for this interference include the laser overheating during the day, and possible optical interference from sunlight entering the well.

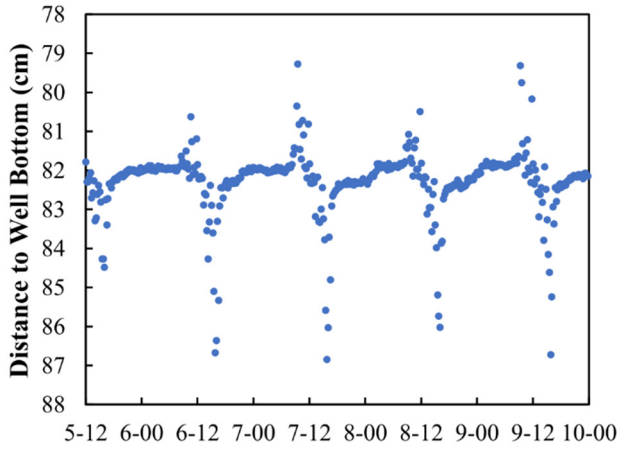


Figure 11. Results from the dry well trial. *Similar to the results from the initial field trial, the dry well trial was fairly linear, with periodic spikes around noon.*

However, due to the interference not occurring from the hours of 12 AM to 5 AM (Figure 12), it does not affect the quality of the ET measurements. A possible reason for this influence is the effect that air temperature can have on the refractive index of air, which could potentially interfere with the measurement accuracy [20].

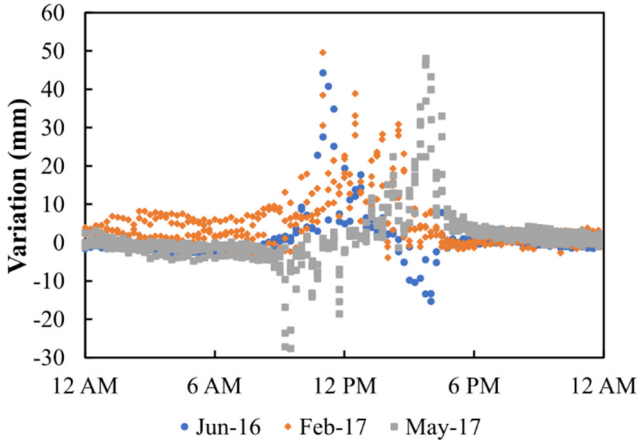


Figure 12. Overall Variation. *When comparing the levels of variation across all three dry trials, it can be seen that the LB-WLS is fairly consistent during the night, but is subject to random noise during the day.*

## IV. Conclusion

Overall, the LB-WLS consistently performed better than the loggers across multiple matrices. It had lower residual noise in the lab trials, and lower RSE values and ET measurements closer to the PET measurements in the field trials. Using either a solar cell or a low power computer such as the LoPy, the LB-WLS has the potential to be deployed in the field indefinitely. Currently, the only impediment is that occasionally, the LB-WLS misfires, which causes the script to time out. This bug has been plaguing the development of the LB-WLS since the early stages, and if solved, would make the LB-WLS a definite contender in the water level sensor field.

## References

[1] M. Jung, M. Reichstein, P. Ciais, S. Seneviratne, J. Sheffield, M. Goulden, G. Bonan, et al. "Recent decline in the global land evapotranspiration trend due to limited moisture supply," *Nature*, vol. 467, no. 7318, pp. 951–954, 2010.

[2] D. McLaughlin, D. Kaplan, and M. Cohen, "Managing Forests for Increased Regional Water Yield in the Southeastern U.S. Coastal Plain," *Journal of the American Water Resouces Association*, vol. 49, no. 4, pp. 953–965, 2013.

[3] Flerchinger, Hanson, and Wight, "Modeling Evapotranspiration and Surface Energy Budgets Across a Watershed," *Water Resources Research*, vol. 32, no. 8, pp. 2539–2548, 1996.

[4] J. Drexler, R. Snyder, D. Spano, and T. Kyaw, "A review of models and micrometeorological methods used to estimate wetland evapotranspiration," *Hydrological Processes*, vol. 18, no. 11, pp. 2071–2101, 2004.

[5] WN White, "A method of estimating ground-water supplies based on discharge by plants and evaporation from soil: Results of investigations in Escalante Valley, Utah," 1932.

[6] D. McLaughlin and M. Cohen, "Thermal artifacts in measurements of fine-scale water level variation," *Water Resources Research*, vol. 47, no. 9, 2011.

[7] S. Cain, G. Davis, S. Loheide, and J. Butler, "Noise in Pressure Transducer Readings Produced by Variations in Solar Radiation," *Groundwater*, vol. 42, no. 6, pp. 939–944, 2004.

[8] J. R. Steenstrup, M. Chun, and K. Hobart, "R2Sonic Pioneers of Wideband High-Resolution Multibeam Systems." 2006.

[9] M.-C. Amann, T. Bosch, M. Lescure, R. Myllyla¨, and M. Rioux, "Laser ranging: a critical review of usual techniques for distance measurement," *Optical Engineering*, vol. 40, no. 1, pp. 10–19, 2001.

[10] SM Nejad and S Olyaee, "Comparison of TOF, FMCW and phase-shift laser range-finding methods by simulation and measurement," *Quarterly Journal of Technology & Education*, 2006.

[11] P. Hu, J. Tan, H. Yang, X. Zhao, and S. Liu, "Phase-shift laser range finder based on high speed and high precision phase-measuring techniques," The 10th International Symposium of Measurement Technology and Intelligent Instruments, 06-Jul-2011.

[12] DSM&T, "IP Rating." 2011.

[13] Leica Geosystems, "Leica DISTO E7100i," 2016.

[14] JD Barchers, "Non-cooperative laser target enhancement system and method," *US Patent 8,076,624 B1*, 2011.

[15] S. Loheide, J. Butler, and S. Gorelick, "Estimation of groundwater consumption by phreatophytes using diurnal water table fluctuations: A saturated-unsaturated flow assessment," *Water Resources Research*, vol. 41, no. 7, p. n/a–n/a, 2005.

[16] HR Duke, "Capillary properties of soils-influence upon specific yield," *Transactions of the ASAE*, 1972.

[17] V. T. Chow, D. R. Maidment, and L. W. Mays, "Applied Hydrology," 1988.

[18] MW Mitchell, "Evaluation of the agricultural field scale irrigation requirement simulation (AFSIRS) in predicting golf course irrigation requirements with site-specific data," 2004.

[19] FDEP, "Paynes Prairie Preserve State Park. APPROVED Unit Management Plan," Florida Department of Environmental Protection, Dec. 2013.

[20] Y. Shim, O.-J. Kwon, H.-Y. Choi, and Y.-G. Han, "Influence of Diverse Atmospheric Conditions on Optical Properties of a Pulse Laser in a Time-of-Flight Laser Range Finder," *Journal of the Optical Society of Korea*, vol. 19, no. 1, pp. 1–6, 2015.